Universality in Ionic Three-Body Systems Near an Ion-Atom Feshbach Resonance

Jacek Gębala,[1,*] Michał Tomza,[1,†] and José P. D'Incao[2,3]
[1]Faculty of Physics, University of Warsaw, Pasteura 5, 02-093 Warsaw, Poland
[2]JILA, NIST, and the Department of Physics, University of Colorado, Boulder, Colorado 80309, USA
[3]Department of Physics, University of Massachusetts Boston, Boston, Massachusetts 02125, USA

(Received 31 October 2025; revised 25 April 2026; accepted 1 June 2026; published 28 July 2026)

We calculate the bound and scattering properties of a system of two neutral atoms and an ion near an ion-atom Feshbach resonance. Our results indicate that long-range ion-atom interactions lead to significant deviations from universal behavior derived from contact or van der Waals potentials. We find that ionic systems display an overall suppression of inelastic transitions leading to recombination rates and lifetimes of Efimov state orders of magnitude larger with respect to those for neutral atoms. We further characterize the dense spectra of triatomic molecular ions with extended lifetimes. Our results provide a deeper insight into the universality and structure of three-body ionic systems and establish them as a promising platform for exploring novel few- and many-body phenomena with long-range interactions.

DOI: 10.1103/r7hw-27wv

Cold mixtures of laser-cooled ions and atoms provide exceptional opportunities for exploring and controlling quantum systems, enabling precise manipulation of both quantum states and collision dynamics [1,2]. These hybrid systems have become a cornerstone of quantum science, with applications spanning quantum simulation [3,4], quantum information processing [5,6], cold controlled chemistry [7–10], and few- and many-body quantum physics [11–14]. Recently, ultracold ion-atom mixtures have been realized in the quantum regime [15,16], enabled by the large mass imbalance between heavy ions and light neutral atoms, which suppresses micromotion-induced heating [17]. This achievement allows controllable interactions near ion-atom Feshbach resonances [16,18,19] through tunability of the s-wave scattering length [20], thereby opening new avenues for investigating complex quantum few- and many-body phenomena governed by long-range ion-atom interactions [21–27] as well as controlling and sympathetic cooling ions using ion-atom confinement-induced resonances [28,29].

Building on this progress, it is important to recognize that ultracold gases are intrinsically shaped by few-body processes. Among these, three-body recombination—a fundamental chemical reaction in which three free atoms react to form a diatomic molecule carrying away the excess energy—is the dominant mechanism driving atomic and molecular losses, thereby limiting both sample lifetimes and achievable densities [30] necessary for the observation of few- and many-body dynamics. Conversely, recombination is not only a loss mechanism but also a powerful diagnostic tool. Its rate and product distribution provide sensitive probes of fundamental quantum effects such as Efimov physics [31–34], enable detailed studies of state-to-state ultracold chemistry [35–40], and serve as a key method for detecting Feshbach resonances in both neutral and ion-atom systems [16,20]. This multifaceted role highlights the potential that recombination has in revealing crucial aspects of few- and many-body quantum dynamics. The growing ability to control ion-atom systems at ultracold temperatures naturally motivates a closer look at how few-body processes and interactions unfold in the presence of the long-range ion-atom interactions.

Classical and semiclassical theories of ion-atom-atom systems have provided valuable insight into three-body recombination at temperatures well above the quantum regime [41–46], establishing a solid foundation for understanding the basic dynamics. With ultracold experiments now pushing deep into the quantum domain, exciting new questions arise that naturally call for a fully quantum mechanical, nonperturbative description. For instance, while the Efimov universality in heteronuclear, neutral systems characterized by short-range interactions is well understood [47,48], the impact of the long-range ion-atom interaction remains largely unexplored, preventing a deeper insight into the structure and dynamics of strongly interacting ionic few-body systems [49]. Equally compelling are opportunities to map out the influence of the long-range interaction on other nonuniversal or chemical aspects like the state distribution of diatomic molecular ions produced by recombination [35–39] and the structure and stability of triatomic molecular ions, which can be potentially created in ion-atom systems.

In this Letter, we investigate universal and nonuniversal aspects of ionic three-body quantum systems composed of

*Contact author: j.gebala@uw.edu.pl
†Contact author: michal.tomza@fuw.edu.pl

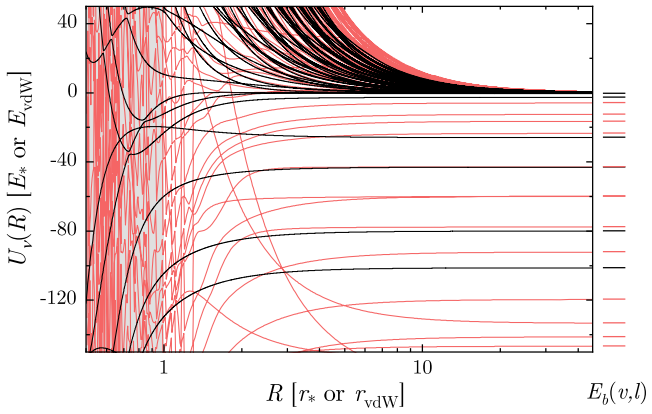

FIG. 1. The three-body hyperspherical potentials $U_\nu(R)$ for the LiLiBa$^+$ (black) and LiLiBa (red) systems calculated at $a_{BX} = 0.1$ (r_* or $r_{\rm vdW}$) for our interaction model supporting six BX s-wave bound states and two BB s-wave bound states. For large R ($R/r_{\rm vdW} \gg 1$ or $R/r_* \gg 1$), potentials $U_\nu(R) > 0$ correspond to three-body continuum channels, describing collisions between three free atoms, while potentials $U_\nu(R) \simeq -E_b(v,l) < 0$ are atom-molecule channels describing collisions between an atom and a molecule. Here, $E_b(v,l)$ denotes the diatomic molecular binding energies of the rovibrational states of the BX and BB interactions. According to the number of the atom-dimer channels in the figure and considering values of $E_{\rm vdW}$ and E_* in absolute units, we estimate the density of diatomic states for the ionic systems to be 100 times larger than for the neutral counterpart.

two identical bosonic atoms, ^{7}Li, and a heavy ion, ^{138}Ba$^+$. Near an ion-atom Feshbach resonance, we find that the ionic system (LiLiBa$^+$) Efimov physics is also manifested in a universal way, but with the three-body recombination rate, L_3, being strongly suppressed compared to its neutral counterpart (LiLiBa) [47]. We also find that the Efimov states in LiLiBa$^+$ possess lifetimes up to 5 orders of magnitude longer than those of LiLiBa, making them more accessible to experimental observation and manipulation. These results confirm that systems with long-range ion-atom interactions belong to a new class of universality [49]. We also show that the product state distribution of recombination for both ionic and neutral systems follows the same $1/E_b$ propensity rule observed in homonuclear systems [35–39], with no significant preference for forming Li_2 or LiBa molecules. Finally, we characterize weakly bound triatomic molecular ions, confirming the high density of states characteristic of long-range ion-atom interactions. Together, these results provide a deeper insight on the universality, stability, and structure of ion-atom systems and establish them as a promising platform for exploring novel few- and many-body phenomena with long-range interactions.

Our investigation of the universality of the ion-atom-atom dynamics begins with the adiabatic hyperspherical representation [34,50,51]. In the hyperspherical representation, the system's internal motion and rotations are described by a set of hyperangles Ω, while its overall size is described by the hyperradius R [34,50,51]. Bound and scattering properties of the system are obtained through solutions of the hyperradial Schrödinger equation

$$\left[-\frac{\hbar^2}{2\mu}\frac{d^2}{dR^2} + U_\nu(R) - E\right]F_\nu(R) + \sum_{\nu'} W_{\nu\nu'}(R)F_{\nu'}(R) = 0, \tag{1}$$

where $\mu = (m_B^2 m_X/M)^{1/2}$ is the three-body reduced mass of a system of two identical bosonic atoms, B, and a third dissimilar atom, X, of masses m_B and m_X, respectively; total mass $M = 2m_B + m_X$; and ν represents the set of quantum numbers characterizing each channel. The hyperradial Schrödinger equation (1) describes the hyperradial motion governed by the three-body effective potentials $W_\nu(R) = U_\nu(R) + W_{\nu\nu}(R)$ supporting bound and resonant states and nonadiabatic couplings $W_{\nu\neq\nu'}(R)$ driving the inelastic transitions between the different channels. Both U_ν and $W_{\nu\nu'}$ are determined via the solutions of the hyperangular Hamiltonian, containing all the interatomic interactions [34,50,51]. In Fig. 1, we display the adiabatic potentials for the LiLiBa and LiLiBa$^+$ systems relevant to our present Letter.

Here, we assume the interactions in the three-body system to be a pairwise sum of the interatomic interactions between the identical bosons (in our case, ^{7}Li), v_{BB}, and that between the bosons and the third particle (Ba or Ba$^+$), v_{BX}. In our interaction model, the interaction between identical bosons is given by the Lennard-Jones potential $v_{BB}(r) = -C_6^B/r^6(1-\lambda_B^6/r^6)$, while for the interspecies interaction, it is given either by a Lennard-Jones potential $v_{BX}(r) = -C_6/r^6(1-\lambda_X^6/r^6)$, in the case of the neutral Li-Ba pair, or by the regularized polarization potential $v_{BX}(r) = -C_4/r^4(1-\lambda_X^4/r^4)$ for the Li-Ba$^+$ pair. Here, C_4 and C_6 are long-range induction and dispersion coefficients [1,52,53], r is the interatomic distance, and λ_B and λ_X parameters are adjusted to produce the desired value of the s-wave scattering length as well as the number of bound states each interaction pair can support. For our studies, the interaction between Li atoms, v_{BB}, is set with $\lambda_B \approx 19.58a_0$, producing two s-wave Li_2 molecular states and the background scattering length of $-27.3a_0$ [54–56], where a_0 is the Bohr radius, while we vary λ_X for v_{BX} to simulate the changes in the interspecies scattering length, a_{BX}, near a Feshbach resonance.

Besides the distinct short- and long-range character of the v_{BX} interaction for neutral and ionic systems, another important distinction is the characteristic length and energy scales defining the onset of universality in the system. While for neutral systems, the relevant scales are determined by the van der Waals length and energy given, respectively, by $r_{\rm vdW} = (2\mu_{BX}C_6/\hbar^2)^{1/4}/2$ and $E_{\rm vdW} = \hbar^2/(2\mu_{BX}r_{\rm vdW}^2)$, where $\mu_{BX} = m_B m_X/(m_B+m_X)$, for the ionic system they are defined by the polarization length and energy, $r_* = (2\mu_{BX}C_4/\hbar^2)^{1/2}/2$ and $E_* = \hbar^2/(2\mu_{BX}r_*^2)$, respectively.

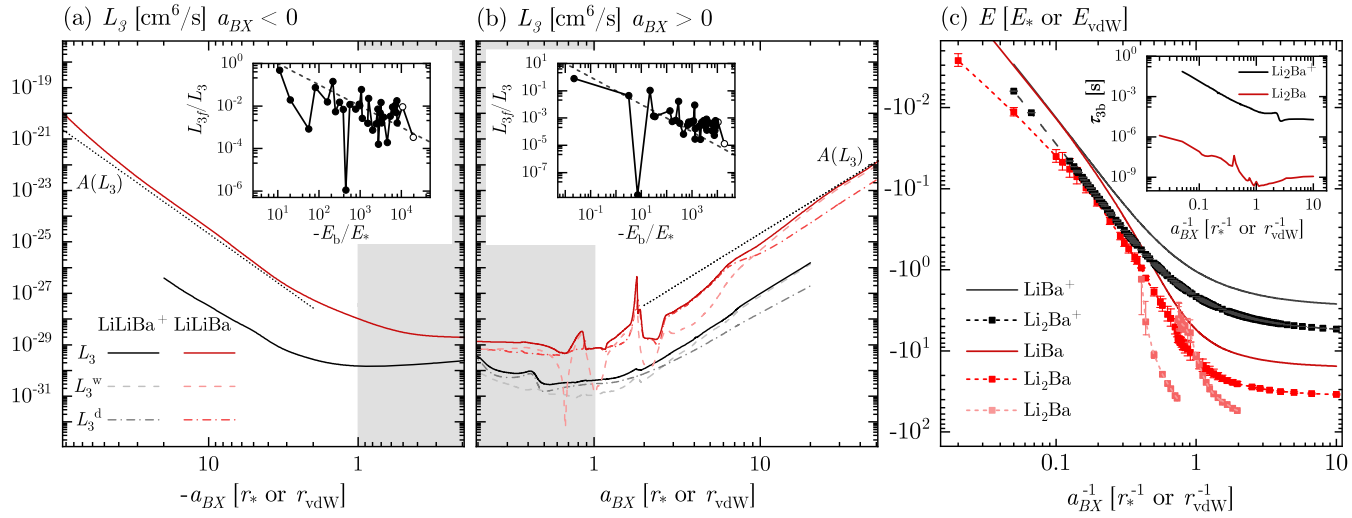

FIG. 2. (a),(b) Three-body recombination rate L_3 and partial rates L_3^w and L_3^d for LiLiBa (red) and LiLiBa$^+$ (black). The results for LiLiBa$^+$ recombination are multiplied by $(r_{vdW}/r_*)^4$ in order to properly compare that with recombination of LiLiBa systems. For small values of $|a_{BX}| \lesssim r_*$ (or r_{vdW}), L_3 display resonant effects associated with high-partial waves diatomic molecular states [60], some of which are not resolved in the figure. Dotted lines represent the amplitude for L_3, $A(L_3)$, from the universal theory [47]. The insets of panels (a) and (b) display the product state distributions of LiLiBa$^+$ recombination, L_{3f}/L_3 [see Eq. (2)], in terms of the molecular final state binding energy, E_b, displaying the $1/E_b$ propensity rule of Ref. [37]. (c) Energy of the lowest Efimov state for LiLiBa (red) and LiLiBa$^+$ (black) and the corresponding width Γ expressed as error bars. Two additional trimer states associated with two-body rotational states (pink) [60] are also presented together with their energies and widths. The inset in (c) shows the lifetime $\tau = \hbar/\Gamma$ of the Efimov states for both LiLiBa and LiLiBa$^+$.

In our system, they are equal to $r_{vdW} \approx 44.99a_0$, $E_{vdW} \approx k_B \times 6409.39$ μK (or $h \times 133.55$ MHz), $r_* \approx 707.03a_0$, and $E_* \approx k_B \times 25.95$ μK (or $h \times 0.54075$ MHz), illustrating the disparate length and energy scales relevant for neutral and ionic systems caused by the strong polarization effects. To ensure the proper comparison between neutral and ionic systems, we express the results for each system in terms of its characteristic length and energy scales whenever appropriate.

For our scattering calculations, we define the three-body recombination constant for a system of two identical bosons at collision energy E as [57]

$$L_3(E) = \sum_J \sum_{f,i} 32\pi^2\hbar \frac{(2J+1)}{\mu k^4} |S_{fi}^J|^2 = \sum_f L_{3f}, \quad (2)$$

with $k = (2\mu E/\hbar^2)^{1/2}$, f running over all final (atom-dimer) channels, and i over the initial (three-body continuum) channels (see Fig. 1). Here, L_{3f} is the partial recombination rate into the final state f and the corresponding S-matrix obtained from the solutions of Eq. (1) using the methodology developed in Ref. [51]. For the regime of ultracold collisions ($E \ll E_{vdW}$ or E_*), we consider only the lowest total three-body angular momentum $J = 0$, as higher partial-waves contributions are suppressed in this regime [58,59].

Figures 2(a) and 2(b) present the three-body recombination rate, L_3, for LiLiBa (red solid lines) and LiLiBa$^+$ (black solid lines) at collision energy $E/k_B = 0.01$ μK as a function of the interspecies scattering lengths, a_{BX}. In the figure, we also show the rate L_3^w for recombination into the weakly bound Feshbach molecular state ($a_{BX} > 0$) as well as recombination into all other deeply bound states, $L_3^d = L_3 - L_3^w$. For the ionic system, we use a Li-Li interaction supporting 2 s-wave states while the Li-Ba$^+$ supports 6 s-wave states (for a total of ∼10 molecular states). For the neutral system, we use both Li-Li and Li-Ba interactions that support 2s-wave states (for a total of ∼40 states). For both ionic and neutral systems, we include in our calculations 50 three-body continuum channels. We estimate our results to be converged within a 1–2% level. In the attempt to gain a better understanding of how recombination proceeds for ionic systems, in the inset of Figs. 2(a) and 2(b), we show the product state distribution L_{3f}/L_3 in terms of the binding energy of the final molecular state, E_b, for both $a_{BX} > 0$ and $a_{BX} < 0$, respectively. Although for LiLiBa$^+$ there are two types of molecular final products ($Li_2 + Ba^+$ or $LiBa^+ + Li$), our results in the inset of Figs. 2(a) and 2(b) verify the same $L_{3f}/L_3 \sim 1/E_b$ propensity rule found for neutral homonuclear ^{87}Rb and ^{85}Rb recombination [35–39], with no preference over Li_2 (open symbol) or $LiBa^+$ (closed symbol) molecular states. This indicates that the same physical processes found for neutral (homonuclear) systems apply to ionic (heteronuclear) systems despite the highly complex nature of the

three-body interactions at short distances ($R \lesssim r_*$ or $R \lesssim r_{\rm vdW}$ in Fig. 1).

For large values of $|a_{BX}|$, $|a_{BX}| \gtrsim r_*$ or $r_{\rm vdW}$, Fig. 2 shows that L_3 follows the expected a_{BX}^4 scaling behavior [34]. Moreover, in this range of a_{BX}, interference and resonant behaviors are expected. They are associated with the nth ($n = 0, 1, 2, \ldots$) Efimov state for $a_{BX} = a_+ e^{n\pi/s_0} > 0$ and $a_{BX} = a_- e^{n\pi/s_0} < 0$, respectively [31–34], with s_0 being the Efimov universal coefficient controlling the strength of the Efimov interaction. As usual, the expected values of three-body parameters $|a_+|$ and $|a_-|$ are typically larger than the characteristic range of the interactions [61]. However, since LiLiBa$^+$ and LiLiBa are both unfavorable mass-imbalanced systems ($m_X/m_B \gg 1$), the Efimov coefficient is small, $s_0 \approx 0.03562$, and geometric scaling extremely large, $e^{\pi/s_0} \approx 2 \times 10^{38}$, in comparison to $s_0 \approx 1.00624$ and $e^{\pi/s_0} \approx 22.7$ for three identical bosons systems. As a result, it is unlikely that such systems will display interference and resonance phenomena for experimentally accessible values of a_{BX}. Nevertheless, universal behavior is still expected for the amplitude of L_3, $L_3^{\rm w}$, and $L_3^{\rm d}$ as shown in Ref. [47]. Such universal results for L_3 (see End Matter) depend on the mass ratio m_X/m_B, a_+, a_-, and η, the nonuniversal inelasticity parameter describing decay to deeply bound molecular states [31,34]. For the LiLiBa neutral system, our numerical calculations for L_3 agree with the universal results of Ref. [47]. The straight lines in Figs. 2(a) and 2(b) represent the amplitude of the universal L_3 without the interference and resonant terms (see End Matter) and are denoted by $A(L_3)$. From the comparison to the universal results we obtain $a_- \approx -200 r_{\rm vdW}$, $\eta \approx 0.17$ for $a_{BX} < 0$, and $\eta \approx 0.027$ for $a_{BX} > 0$.

For LiLiBa$^+$, we could not identify any reasonable set of parameters a_+, a_-, and η within the framework of the universal theory [47] that reproduces the recombination amplitude shown in Fig. 2. Furthermore, by employing different interaction models for the Li-Ba$^+$ potential—each supporting a different number of bound states—we confirm that our results for the LiLiBa$^+$ system are themselves universal, yet suppressed by a factor of about 250 compared to the corresponding universal predictions of Ref. [47]. We attribute this suppression of inelastic transitions to the difference in how the LiLiBa$^+$ interactions change as R approaches short distances compared to the LiLiBa case. As shown in Fig. 1, the three-body potentials for LiLiBa$^+$ vary more slowly approaching short distances than those for LiLiBa, leading to smaller nonadiabatic couplings $W_{\nu\nu'}$ in Eq. (1) and suppressing inelastic transitions. We have verified this reduction of nonadiabatic couplings numerically.

Evidently, these findings raise the question of what makes the universality for ionic systems different than that of neutral atoms. In fact, as shown in Ref. [49], systems interacting via $1/r^6$ and $1/r^4$ interactions (in our case, the LiLiBa and LiLiBa$^+$ systems, respectively) belong to different universality classes and are characterized by different values of the universal three-body parameters (e.g., a_-) [62]. Although the universal theory [47]—constructed within the framework of the effective-field theory (EFT) assuming contact, zero-range interactions—does not provide the values of the three-body parameters, they provide universal expressions for L_3 in terms of such three-body parameters as well as various universal relationships between them. The validity of these expressions has been extensively verified for neutral atomic systems belonging to the $1/r^6$ universality class. Nevertheless, systems within the $1/r^4$ universality class have fundamentally different low-energy properties manifested, for instance, via the effective-range expansion [63–66]. We provide a detailed analysis of the difference between the effective range expansion for both $1/r^6$ and $1/r^4$ interactions in the End Matter. Such modifications of the low-energy behavior suggest that changes to the universal EFT are required in order to properly describe the universality of ionic three-body systems, similar to those in Refs. [67,68], which demonstrate the importance of treating $1/r^6$ and $1/r^4$ interactions within the EFT framework. Our results on the changes observed in our L_3 calculations for neutral and ionic systems, along with the $1/r^4$ universality class studies of Ref. [49], indicate that the ionic nature of the two-body interaction affects not only the universality of the three-body parameter but also the universal collision rates and other universal relationships derived from the EFT framework [47]. We provide a detailed analysis of the mechanisms of the ion-atom-atom universality in Supplemental Material [69].

Although both the LiLiBa and LiLiBa$^+$ systems are unfavorable for Efimov physics (due to the value of the Efimov coefficient, $s_0 \approx 0.03562$), our calculations in Fig. 2(c) show that for $a_{BX} > 0$, the Efimov ground state remains bound for values of $a_{BX}/r_{\rm vdW}$ and a_{BX}/r_* much smaller than $e^{\pi/s_0} \approx 2 \times 10^{38}$. This can be explained by the variational principle of Ref. [74], which states that the ground state binding energy of a triatomic molecule can not exceed three times that of the diatomic molecule, preventing the Efimov ground state from crossing the atom-dimer threshold and becoming unbound [75,76]. In Fig. 2(c), we show the diatomic molecular energies of the corresponding Feshbach states, $E_{\rm 2b}^*$ (solid lines), along with the energies $E_{\rm 3b}$ (dashed lines with symbols) and width $\Gamma_{\rm 3b}$ (error bars) of the triatomic molecular states obtained via the time-delay calculations similar to that of Ref. [77]. While the energies of the Efimov ground state for the LiLiBa and LiLiBa$^+$ systems are similar (in relative units), their corresponding lifetimes $\tau_{\rm 3b} = \hbar/\Gamma_{\rm 3b}$ are substantially different. The Efimov LiLiBa$^+$ ground state has a lifetime around 5 orders of magnitude longer than those of LiLiBa [see the inset of Fig. 2(c)], with lifetimes as long as 100 ms for the range of a_{BX} shown in Fig. 2(c). The longer lifetimes for LiLiBa$^+$ states can be understood by the combination of their more weakly bound nature compared to the LiLiBa states—determined by the ratio of characteristic energy scales, $E_*/E_{\rm vdW} \approx 4.05 \times 10^{-3}$)—and the suppression by a factor of 250 of the inelastic transitions for LiLiBa$^+$ [see

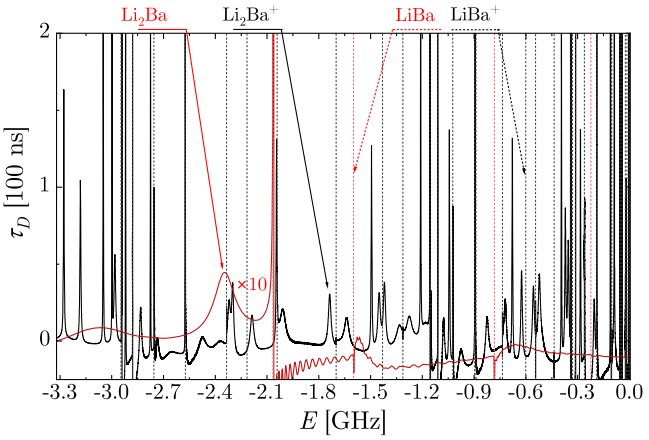

FIG. 3. The time delay for ^{7}Li^{7}Li^{138}Ba (red) and ^{7}Li^{7}Li^{138}Ba$^+$ (black) calculated for $a_{BX} = 0.1$ (r_* or $r_{\rm vdW}$). The results for the neutral system have been multiplied by a factor of 10. The vertical dashed lines are the energies of two-body molecular states to which the effective potentials $W_\nu(R)$ converge at large values of R. The peaks and width of the time-delay parameter describe the energies and lifetimes of the three-body bound states supported by $W_\nu(R)$.

Figs. 2(a) and 2(b)], thus leading to an overall factor of $E_*/E_{\rm vdW}/250 \approx 1.62 \times 10^{-5}$. Long-lived ground Efimov states in neutral atoms have so far remained elusive, making ionic Efimov states likely to produce interesting regimes in the ultracold ion-atom gas mixture. While ionic Efimov states are extremely weakly bound ($|E_{3b}| \ll E_* \approx 25.95$ μK for LiLiBa$^+$) and difficult to populate due to the still limited temperatures experiments can reach, their extremely large extent, $\langle R \rangle_{3b} \gg r_*$, can exceed the average interatomic distances (approximately 30 r_* for densities around 10^{12} cm^{-3}), potentially leading to novel physical regimes [3–5,11,21–24,78].

To further explore binding phenomena in ionic few-body states and the differences to neutral atom systems, we also calculated the energy spectrum and the corresponding lifetimes of the triatomic molecular states beyond the energy range relevant for Efimov physics, i.e., $E > E_{\rm vdW} \approx h \times 133.55$ MHz for LiLiBa and $E > E_* \approx h \times 0.54075$ MHz for LiLiBa$^+$. Figure 3 shows our calculations of the time delay $\tau_D(E)$ [77] for a broad range of energies (from 0 to $h \times 3.3$ GHz), with molecular energies E_r determined through the values of E in which $\tau_D(E)$ is maximal, i.e., $d\tau_D(E)/dE = 0$, and corresponding lifetimes given by $\tau_r = \tau_D(E_r)/4$. Figure 3 shows that, similar to the diatomic case (see caption of Fig. 1), the energy spectrum of triatomic molecular ions (black curve) is also much denser than that of the neutral system (red curve). [Note that in Fig. 3, the vertical dashed lines indicate the energy of the LiBa (red) and LiBa$^+$ (black) molecular states.]

Our calculations in Fig. 3 show that the Li_2Ba three-body molecular states have significantly shorter lifetimes than typical Li_2Ba^+ molecular states. Notably, certain states in the ionic system are unusually narrow. Such states are characterized by slightly increased lifetimes for lower binding energies, ranging from 1 to 10 μs.

In summary, we investigated universal and nonuniversal aspects of ionic three-body systems composed of two identical bosonic atoms, ^{7}Li, and a heavy ion, ^{138}Ba$^+$. We found that near an ion-atom Feshbach resonance, the ionic system (LiLiBa$^+$) exhibits Efimov physics in close analogy to its neutral counterpart (LiLiBa), but with the recombination rate, L_3, strongly suppressed compared to the neutral case [47], suggesting that the long-range ion-atom interaction defines a class of universality where both universal three-body parameters [49] and their universal relationships are distinct from universality for neutral atom systems [47]. We characterized the energy and lifetime of Efimov ground state in both LiLiBa$^+$ and LiLiBa systems and found that the lifetime of the ionic Efimov state is 5 orders of magnitude longer than its neutral counterpart, consistent with the difference in characteristic energy scales ($E_{\rm vdW}$ and E_*) and the suppression factor found for the ionic L_3. We also characterized weakly bound triatomic molecular ions, confirming the expected high density of states characteristic of long-range ion-atom interactions. The generally longer lifetimes of ion-atom-atom systems constitute a key advantage for future experiments, opening new avenues to explore few- and many-body effects in ultracold ion-atom systems.

An interesting pathway for future research involves the description of the dependence of universality for ionic systems on the narrowness of Feshbach resonance. The departure from the usual universal behavior in Efimov physics near narrow Feshbach resonances stems from the appearance of a new, large, two-body length scale associated with the effective range, which leads to modifications of the long-range behavior of the Efimov interactions [79–84]. Taking into account the relevant length scales, r_*, we do expect similar effects in ionic systems.

Acknowledgments—The authors thank Hans-Werner Hammer for fruitful discussions. We gratefully acknowledge the National Science Centre Poland (Grants No. 2020/38/E/ST2/00564 and No. 2023/49/N/ST2/03439) for financial support and Poland's high-performance computing infrastructure PLGrid (HPC Centers: ACK Cyfronet AGH) for providing computer facilities and support (computational Grant No. PLG/2024/017527). J. P. D. also acknowledges partial support from the U.S. National Science Foundation, Grant No. PHY-2452751, and NASA/JPL 1502690. This research was supported in part by the National Science Foundation under Grant No. NSF PHY-1748958 to the Kavli Institute for Theoretical Physics (KITP).

Data availability—The data that support the findings of this article are openly available [85].

[1] M. Tomza, K. Jachymski, R. Gerritsma, A. Negretti, T. Calarco, Z. Idziaszek, and P. S. Julienne, Cold hybrid ion-atom systems, Rev. Mod. Phys. **91**, 035001 (2019).

[2] M. Deiß, S. Willitsch, and J. Hecker Denschlag, Cold trapped molecular ions and hybrid platforms for ions and neutral particles, Nat. Phys. **20**, 713 (2024).

[3] U. Bissbort, D. Cocks, A. Negretti, Z. Idziaszek, T. Calarco, F. Schmidt-Kaler, W. Hofstetter, and R. Gerritsma, Emulating solid-state physics with a hybrid system of ultracold ions and atoms, Phys. Rev. Lett. **111**, 080501 (2013).

[4] K. Jachymski and A. Negretti, Quantum simulation of extended polaron models using compound atom-ion systems, Phys. Rev. Res. **2**, 033326 (2020).

[5] H. Doerk, Z. Idziaszek, and T. Calarco, Atom-ion quantum gate, Phys. Rev. A **81**, 012708 (2010).

[6] L. Ratschbacher, C. Sias, L. Carcagni, J. M. Silver, C. Zipkes, and M. Köhl, Decoherence of a single-ion qubit immersed in a spin-polarized atomic bath, Phys. Rev. Lett. **110**, 160402 (2013).

[7] L. Ratschbacher, C. Zipkes, C. Sias, and M. Köhl, Controlling chemical reactions of a single particle, Nat. Phys. **8**, 649 (2012).

[8] T. Sikorsky, Z. Meir, R. Ben-Shlomi, N. Akerman, and R. Ozeri, Spin-controlled atom–ion chemistry, Nat. Commun. **9**, 920 (2018).

[9] A. D. Dörfler, P. Eberle, D. Koner, M. Tomza, M. Meuwly, and S. Willitsch, Long-range versus short-range effects in cold molecular ion-neutral collisions, Nat. Commun. **10**, 5429 (2019).

[10] H. Hirzler, R. S. Lous, E. Trimby, J. Pérez-Ríos, A. Safavi-Naini, and R. Gerritsma, Observation of chemical reactions between a trapped ion and ultracold Feshbach dimers, Phys. Rev. Lett. **128**, 103401 (2022).

[11] R. Côté, V. Kharchenko, and M. D. Lukin, Mesoscopic molecular ions in Bose-Einstein condensates, Phys. Rev. Lett. **89**, 093001 (2002).

[12] A. Härter, A. Krükow, A. Brunner, W. Schnitzler, S. Schmid, and J. Hecker Denschlag, Single ion as a three-body reaction center in an ultracold atomic gas, Phys. Rev. Lett. **109**, 123201 (2012).

[13] J. M. Schurer, A. Negretti, and P. Schmelcher, Unraveling the structure of ultracold mesoscopic collinear molecular ions, Phys. Rev. Lett. **119**, 063001 (2017).

[14] K. S. Kleinbach, F. Engel, T. Dieterle, R. Löw, T. Pfau, and F. Meinert, Ionic impurity in a Bose-Einstein condensate at submicrokelvin temperatures, Phys. Rev. Lett. **120**, 193401 (2018).

[15] T. Feldker, H. Fürst, H. Hirzler, N. Ewald, M. Mazzanti, D. Wiater, M. Tomza, and R. Gerritsma, Buffer gas cooling of a trapped ion to the quantum regime, Nat. Phys. **16**, 413 (2020).

[16] P. Weckesser, F. Thielemann, D. Wiater, A. Wojciechowska, L. Karpa, K. Jachymski, M. Tomza, T. Walker, and T. Schaetz, Observation of Feshbach resonances between a single ion and ultracold atoms, Nature (London) **600**, 429 (2021).

[17] M. Cetina, A. T. Grier, and V. Vuletić, Micromotion-induced limit to atom-ion sympathetic cooling in Paul traps, Phys. Rev. Lett. **109**, 253201 (2012).

[18] F. Thielemann, J. Siemund, D. von Schoenfeld, W. Wu, P. Weckesser, K. Jachymski, T. Walker, and T. Schaetz, Exploring atom-ion Feshbach resonances below the *s*-wave limit, Phys. Rev. X **15**, 011051 (2025).

[19] M. Morita, J. Siemund, W. Wu, D. von Schoenfeld, J. Grieshaber, A. Wojciechowska, K. Jachymski, T. Walker, F. Thielemann, T. Schaetz, and M. Tomza, Magnetic Feshbach resonances in $Ba^+ + Li$ collisions due to strong spin-orbit coupling, arXiv:2507.12936.

[20] C. Chin, R. Grimm, P. Julienne, and E. Tiesinga, Feshbach resonances in ultracold gases, Rev. Mod. Phys. **82**, 1225 (2010).

[21] W. Casteels, J. Tempere, and J. T. Devreese, Polaronic properties of an ion in a Bose-Einstein condensate in the strong-coupling limit, J. Low Temp. Phys. **162**, 266 (2011).

[22] H. Hirzler, E. Trimby, R. S. Lous, G. C. Groenenboom, R. Gerritsma, and J. Pérez-Ríos, Controlling the nature of a charged impurity in a bath of Feshbach dimers, Phys. Rev. Res. **2**, 033232 (2020).

[23] G. E. Astrakharchik, L. A. Peña Ardila, R. Schmidt, K. Jachymski, and A. Negretti, Ionic polaron in a Bose-Einstein condensate, Commun. Phys. **4**, 94 (2021).

[24] E. R. Christensen, A. Camacho-Guardian, and G. M. Bruun, Charged polarons and molecules in a Bose-Einstein condensate, Phys. Rev. Lett. **126**, 243001 (2021).

[25] S. Ding, M. Drewsen, J. J. Arlt, and G. M. Bruun, Mediated interaction between ions in quantum degenerate gases, Phys. Rev. Lett. **129**, 153401 (2022).

[26] G. E. Astrakharchik, L. A. Peña Ardila, K. Jachymski, and A. Negretti, Many-body bound states and induced interactions of charged impurities in a bosonic bath, Nat. Commun. **14**, 1647 (2023).

[27] R. Pessoa, S. A. Vitiello, and L. A. Peña Ardila, Fermi polaron in atom-ion hybrid systems, Phys. Rev. Lett. **133**, 233002 (2024).

[28] V. S. Melezhik, Z. Idziaszek, and A. Negretti, Impact of ion motion on atom-ion confinement-induced resonances in hybrid traps, Phys. Rev. A **100**, 063406 (2019).

[29] V. S. Melezhik, Improving efficiency of sympathetic cooling in atom-ion and atom-atom confined collisions, Phys. Rev. A **103**, 053109 (2021).

[30] T. Weber, J. Herbig, M. Mark, H.-C. Nägerl, and R. Grimm, Three-body recombination at large scattering lengths in an ultracold atomic gas, Phys. Rev. Lett. **91**, 123201 (2003).

[31] E. Braaten and H.-W. Hammer, Universality in few-body systems with large scattering length, Phys. Rep. **428**, 259 (2006).

[32] C. H. Greene, P. Giannakeas, and J. Pérez-Ríos, Universal few-body physics and cluster formation, Rev. Mod. Phys. **89**, 035006 (2017).

[33] P. Naidon and S. Endo, Efimov physics: a review, Rep. Prog. Phys. **80**, 056001 (2017).

[34] J. P. D'Incao, Few-body physics in resonantly interacting ultracold quantum gases, J. Phys. B **51**, 043001 (2018).

[35] J. Wolf, M. Deiß, A. Krükow, E. Tiemann, B. P. Ruzic, Y. Wang, J. P. D'Incao, P. S. Julienne, and J. Hecker Denschlag, State-to-state chemistry for three-body recombination in an ultracold rubidium gas, Science **358**, 921 (2017).

[36] S. Haze, J. P. D'Incao, D. Dorer, M. Deiß, E. Tiemann, P. S. Julienne, and J. Hecker Denschlag, Spin-conservation propensity rule for three-body recombination of ultracold Rb atoms, Phys. Rev. Lett. **128**, 133401 (2022).

[37] S. Haze, J. P. D'Incao, D. Dorer, J. Li, M. Deiß, E. Tiemann, P. S. Julienne, and J. Hecker Denschlag, Energy scaling of the product state distribution for three-body recombination of ultracold atoms, Phys. Rev. Res. **5**, 013161 (2023).

[38] S. Haze, J.-L. Li, D. Dorer, J. D'Incao, P. S. Julienne, E. Tiemann, M. Deiß, and J. Hecker Denschlag, Controlling few-body reaction pathways using a Feshbach resonance, Nat. Phys. **21**, 228 (2025).

[39] J.-L. Li, P. S. Julienne, J. Hecker Denschlag, and J. P. D'Incao, Spin hierarchy in van der Waals molecule formation via ultracold three-body recombination, Phys. Rev. A **111**, 013308 (2025).

[40] D. Dorer, S. Haze, J.-L. Li, J. P. D'Incao, E. Tiemann, P. S. Julienne, M. Deiß, and J. Hecker Denschlag, Steering reaction flux by coupling product channels, Phys. Rev. Lett. **136**, 063401 (2026).

[41] J. Pérez-Ríos, S. Ragole, J. Wang, and C. H. Greene, Comparison of classical and quantal calculations of helium three-body recombination, J. Chem. Phys. **140**, 044307 (2014).

[42] J. Pérez-Ríos and C. H. Greene, Communication: Classical threshold law for ion-neutral-neutral three-body recombination, J. Chem. Phys. **143**, 041105 (2015).

[43] J. Pérez-Ríos and C. H. Greene, Universal temperature dependence of the ion-neutral-neutral three-body recombination rate, Phys. Rev. A **98**, 062707 (2018).

[44] J. Pérez-Ríos, Cold chemistry: A few-body perspective on impurity physics of a single ion in an ultracold bath, Mol. Phys. **119**, e1881637 (2021).

[45] M. Mirahmadi and J. Pérez-Ríos, Three-body recombination in physical chemistry, Int. Rev. Phys. Chem. **41**, 233 (2022).

[46] M. Londoño, J. Madroñero, and J. Pérez-Ríos, Cold atom-ion systems in radio-frequency multipole traps: Event-driven molecular dynamics and stochastic simulations, Phys. Rev. A **108**, 053324 (2023).

[47] K. Helfrich, H.-W. Hammer, and D. S. Petrov, Three-body problem in heteronuclear mixtures with resonant interspecies interaction, Phys. Rev. A **81**, 042715 (2010).

[48] Y. Wang, J. Wang, J. P. D'Incao, and C. H. Greene, Universal three-body parameter in heteronuclear atomic systems, Phys. Rev. Lett. **109**, 243201 (2012).

[49] P. Naidon, S. Endo, and M. Ueda, Microscopic origin and universality classes of the Efimov three-body parameter, Phys. Rev. Lett. **112**, 105301 (2014).

[50] H. Suno, B. D. Esry, C. H. Greene, and J. P. Burke, Three-body recombination of cold helium atoms, Phys. Rev. A **65**, 042725 (2002).

[51] J. Wang, J. P. D'Incao, and C. H. Greene, Numerical study of three-body recombination for systems with many bound states, Phys. Rev. A **84**, 052721 (2011).

[52] A. Derevianko, W. R. Johnson, M. S. Safronova, and J. F. Babb, High-precision calculations of dispersion coefficients, static dipole polarizabilities, and atom-wall interaction constants for alkali-metal atoms, Phys. Rev. Lett. **82**, 3589 (1999).

[53] B. Jeziorski, R. Moszynski, and K. Szalewicz, Perturbation theory approach to intermolecular potential energy surfaces of van der waals complexes, Chem. Rev. **94**, 1887 (1994).

[54] A. J. Moerdijk, W. C. Stwalley, R. G. Hulet, and B. J. Verhaar, Negative scattering length of ultracold ^{7}Li gas, Phys. Rev. Lett. **72**, 40 (1994).

[55] E. R. I. Abraham, W. I. McAlexander, C. A. Sackett, and R. G. Hulet, Spectroscopic determination of the s-wave scattering length of lithium, Phys. Rev. Lett. **74**, 1315 (1995).

[56] S. E. Pollack, D. Dries, M. Junker, Y. P. Chen, T. A. Corcovilos, and R. G. Hulet, Extreme tunability of interactions in a ^{7}Li Bose-Einstein condensate, Phys. Rev. Lett. **102**, 090402 (2009).

[57] N. P. Mehta, S. T. Rittenhouse, J. P. D'Incao, J. von Stecher, and C. H. Greene, General theoretical description of n-body recombination, Phys. Rev. Lett. **103**, 153201 (2009).

[58] B. D. Esry, C. H. Greene, and H. Suno, Threshold laws for three-body recombination, Phys. Rev. A **65**, 010705(R) (2001).

[59] J. P. D'Incao and B. D. Esry, Scattering length scaling laws for ultracold three-body collisions, Phys. Rev. Lett. **94**, 213201 (2005).

[60] J. Wang, J. P. D'Incao, Y. Wang, and C. H. Greene, Universal three-body recombination via resonant d-wave interactions, Phys. Rev. A **86**, 062511 (2012).

[61] J. Wang, J. P. D'Incao, B. D. Esry, and C. H. Greene, Origin of the three-body parameter universality in Efimov physics, Phys. Rev. Lett. **108**, 263001 (2012).

[62] From this perspective, our results for LiLiBa and LiLiBa$^+$ systems partially confirm university classes classification of [49], since we found that L_3 for LiLiBa is expected to display an Efimov resonance at $a_{BX} = a_- \approx -200 r_{\mathrm{vdW}}$ while LiLiBa$^+$ does not [see Fig. 2(a)].

[63] V. V. Flambaum, G. F. Gribakin, and C. Harabati, Analytical calculation of cold-atom scattering, Phys. Rev. A **59**, 1998 (1999).

[64] H. R. Sadeghpour, J. L. Bohn, M. J. Cavagnero, B. D. Esry, I. I. Fabrikant, J. H. Macek, and A. R. P. Rau, Collisions near threshold in atomic and molecular physics, J. Phys. B **33**, R93 (2000).

[65] T. F. O'Malley, L. Rosenberg, and L. Spruch, Low-energy scattering of a charged particle by a neutral polarizable system, Phys. Rev. **125**, 1300 (1962).

[66] S. J. Buckman and J. Mitroy, Analysis of low-energy electron scattering cross sections via effective-range theory, J. Phys. B **22**, 1365 (1989).

[67] D. Odell, A. Deltuva, and L. Platter, Van der waals interaction as the starting point for an effective field theory, Phys. Rev. A **104**, 023306 (2021).

[68] D. Odell, D. R. Phillips, and U. van Kolck, Effective field theory for the bound states and scattering of a heavy charged particle and a neutral atom, Phys. Rev. A **108**, 062817 (2023).

[69] See Supplemental Material at http://link.aps.org/supplemental/10.1103/r7hw-27wv for the detailed discussion on universality in the ion-atom-atom system and complementary results, which includes Refs. [70–73].

[70] J. P. D'Incao and B. D. Esry, Manifestations of the Efimov effect for three identical bosons, Phys. Rev. A **72**, 032710 (2005).

[71] Y. Wang, J. P. D'Incao, and B. D. Esry, Cold three-body collisions in hydrogen–hydrogen–alkali-metal atomic systems, Phys. Rev. A **83**, 032703 (2011).
[72] S. Häfner, J. Ulmanis, E. D. Kuhnle, Y. Wang, C. H. Greene, and M. Weidemüller, Role of the intraspecies scattering length in the Efimov scenario with large mass difference, Phys. Rev. A **95**, 062708 (2017).
[73] K. Oi, P. Naidon, and S. Endo, Universality of Efimov states in highly mass-imbalanced cold-atom mixtures with van der Waals and dipole interactions, Phys. Rev. A **110**, 033305 (2024).
[74] L. W. Bruch and K. Sawada, Inequality relating the ground-state energies of two and three bosons, Phys. Rev. Lett. **30**, 25 (1973).
[75] M. D. Lee, T. Köhler, and P. S. Julienne, Excited Thomas-Efimov levels in ultracold gases, Phys. Rev. A **76**, 012720 (2007).
[76] P. M. A. Mestrom, J. Wang, C. H. Greene, and J. P. D'Incao, Efimov–van der Waals universality for ultracold atoms with positive scattering lengths, Phys. Rev. A **95**, 032707 (2017).
[77] E. Nielsen, H. Suno, and B. D. Esry, Efimov resonances in atom-diatom scattering, Phys. Rev. A **66**, 012705 (2002).
[78] R. Gerritsma, A. Negretti, H. Doerk, Z. Idziaszek, T. Calarco, and F. Schmidt-Kaler, Bosonic Josephson junction controlled by a single trapped ion, Phys. Rev. Lett. **109**, 080402 (2012).
[79] D. S. Petrov, Three-boson problem near a narrow Feshbach resonance, Phys. Rev. Lett. **93**, 143201 (2004).
[80] A. O. Gogolin, C. Mora, and R. Egger, Analytical solution of the bosonic three-body problem, Phys. Rev. Lett. **100**, 140404 (2008).
[81] R. Schmidt, S. P. Rath, and W. Zwerger, Efimov physics beyond universality, Eur. Phys. J. B **85**, 386 (2012).
[82] Y. Wang, J. P. D'Incao, and B. D. Esry, Ultracold three-body collisions near narrow Feshbach resonances, Phys. Rev. A **83**, 042710 (2011).
[83] Y. Yudkin, R. Elbaz, J. P. D'Incao, P. S. Julienne, and L. Khaykovich, Reshaped three-body interactions and the observation of an Efimov state in the continuum, Nat. Commun. **15**, 2127 (2024).
[84] C. Langmack, R. Schmidt, and W. Zwerger, Efimov states near a Feshbach resonance and the limits of van der Waals universality at finite background scattering length, Phys. Rev. A **97**, 033623 (2018).
[85] J. Gębala, M. Tomza, and J. P. D'Incao, 10.5281/zenodo.20513938 (2026).
[86] A. Calle Cordón and E. Ruiz Arriola, Low-energy universality and scaling of van der Waals forces, Phys. Rev. A **81**, 044701 (2010).
[87] B. R. Levy and J. B. Keller, Low-energy expansion of scattering phase shifts for long-range potentials, J. Math. Phys. (N.Y.) **4**, 54 (1963).
[88] L. Spruch, T. F. O'Malley, and L. Rosenberg, Modification of effective-range theory in the presence of a long-range potential, Phys. Rev. Lett. **5**, 375 (1960).

End Matter

Effective range theory—Effective range theory is an important tool for the analysis of low-energy scattering. It became an essential framework for development of the universal theory of ultracold collisions. Effective range theory provides the leading terms in the expansion of $k^{2l+1}\cot\delta_l$ as a function of the collision energy, where δ_l is the phase shift of the scattering wave function for the angular momentum l, and k is the wave number. For collision energies approaching the s-wave regime, we consider only $l=0$. In this regime, the shape-independent approximation to effective range expansion becomes

$$k\cot\delta_0 = -\frac{1}{a}+\frac{1}{2}r_{\mathrm{eff}}k^2+\mathcal{O}(k^4), \tag{A1}$$

which is valid for $k < r_{\mathrm{eff}}{}^{-1}$, where r_{eff} is the effective range and where a is the two-body scattering length. Equation (A1) is valid only for short-range potentials, which fall off faster than any power of $1/r$. The terms of the expansion are modified for inverse power-law potentials, i.e., $v(r)\to -C_n/r^n, r\to\infty$. Nevertheless, if the potentials decay sufficiently rapidly at large r, only the higher order terms are modified. For example, the term $\mathcal{O}(k^4)$ changes to $\mathcal{O}[k^4\ln(k)]$ for $n=6$ [86,87].

The form of solutions of the free and regular radial Schrödinger equation at $k=0$ allows us to approximate the effective range with an energy-independent expression

$$r_{\mathrm{eff}}(a) = 2\int_0^\infty [v_0^2(r)-u_0^2(r)]\mathrm{d}r, \tag{A2}$$

where $v_0(r)=1-r/a$ is the solution to the free radial Schrödinger equation, and $u_0(r)$ is the solution to the Schrödinger equation with a finite potential $V(r)$ [63,65]. However, Eq. (A2) can be obtained only by approximating the solutions at finite k to v_0 and u_0 at short range and setting the value of the integral to 0 at long range, where the two-body potential effectively vanishes. This assumption is valid only for a certain class of long-range two-body potentials of the form $V(r)\to -C_n/r^n, r\to\infty$, where $n>4$.

Long-range potentials, like the ones representing the ion-atom induction dominating interaction at $n=4$, require a more general approach, which introduces terms proportional to $\sim k$ and $\sim k^2\ln k$ in the $k\cot\delta_0$ expansion [88]

$$k\cot\delta_0 = -\frac{1}{a}+c_1^*(a)k+\frac{16r_*^2}{3a}k^2\ln\left(\frac{r_*k}{2}\right) + \frac{1}{2}R_{\mathrm{eff}}^*(a)k^2+\mathcal{O}(k^3), \tag{A3}$$

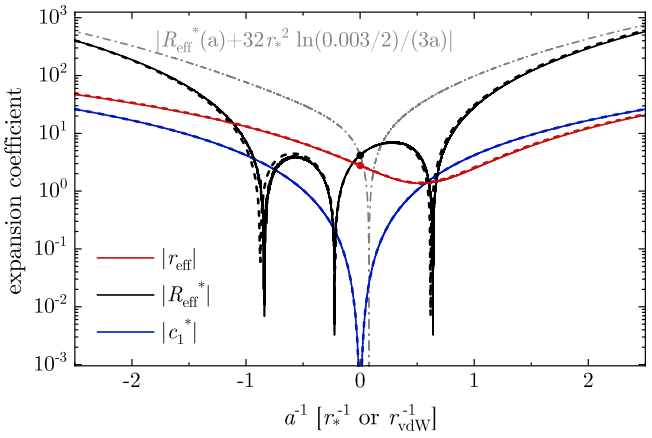

FIG. 4. The (generalized) effective ranges for the ion-atom (black solid line) and neutral (red solid line) two-body interactions. The coefficient $\sim k$ obtained for the ionic expansion is marked as c_1^* (blue solid line). Dashed lines represent the analytical expressions given by Eq. (34) of Ref. [20] for the neutral interaction (red), the expression for $c_1^*(a)$ (blue), and the expression given by Eq. (A4), in which we set $r_{\rm eff}^* = 0$ (black) for the ion-atom interaction. The gray dot-dashed line shows the generalized ionic effective range plus the estimated logarithmic term at $k = 0.003 r_*^{-1}$.

where $c_1^*(a) = 4\pi r_*^2/(3a^2)$ and where

$$R_{\rm eff}^*(a) = r_{\rm eff}^* + \frac{4\pi r_*}{3} + \frac{160 r_*^2}{9a} - \frac{64\psi(\frac{3}{2}) r_*^2}{3a} - \frac{16\pi r_*^3}{3a^2} - \frac{32\pi^2 r_*^4}{9a^3} \tag{A4}$$

is the *generalized* effective range for the ion-atom interaction. In the above equation, we define $r_{\rm eff}^*$ to be the ion-atom effective range. We relate the modifications in the ionic $k\cot\delta_0$ expansion to corresponding changes in the universal theory of few-body collisions arising from long-range interactions.

We present the calculated results for the $k\cot\delta_0$ expansion in Fig. 4. For neutral and ion-atom interactions, we fit the expressions in Eqs. (A1) and (A3), respectively, to numerically obtained values of $k\cot\delta_0$. The coefficients of the effective range expansion are plotted against $1/a$ in units rescaled for both the neutral and ion-atom interactions. The results for the neutral $\sim k^2$ coefficient, i.e., $r_{\rm eff}$, agree with the analytical expression reported in Ref. [20]. Likewise, the ionic $\sim k$ coefficient accurately reproduces the expected $1/a^2$ dependence. For the ion-atom system, the $\sim k^2$ coefficient is extracted by subtracting the logarithmic term from $k\cot\delta_0$ prior to fitting. Specifically, we evaluate the $\sim \ln k$ contribution at $k = 0.003 r_*^{-1}$. At this value, $k\cot\delta_0$ converges to $-1/a$, confirming the correct threshold behavior. The numerical values are compared to Eq. (A4) under the approximation $r_{\rm eff}^* \approx 0$. Any deviations from this formula provide an estimate of the ion-atom effective range. Because the nonlinear $\sim \ln k^2$ term reduces the numerical stability of the fit, we assess its influence by adding it to the $\sim k^2$ coefficient after the fitting procedure. This term has a significant impact on the $\sim k^2$ behavior of the $k\cot\delta_0$ function.

Three-body recombination for $a_{BX} > 0$—The LiLiBa system has a large mass imbalance measured by $\delta = m_X/m_B$, where m_X is the mass of one dissimilar atom X, in our case the barium atom, while the two lithium atoms have masses m_B. We modify the implementation of the universal theory to the three-body problem for large scattering lengths to account for the heteronuclear properties of our system. Following Ref. [47], the rate $L_3^{\rm w}$ for recombination into the weakly bound Feshbach molecular state ($a_{BX} > 0$) is given by

$$L_3^{\rm w} = 2C(\delta)\frac{D(\sin^2[s_0\ln(a_{BX}/a_+)] + \sinh^2(\eta))}{\sinh^2(\pi s_0 + \eta) + \cos^2[s_0\ln(a_{BX}/a_+)]}\frac{\hbar a_{BX}^4}{m_X}, \tag{B1}$$

where $D = 128\pi^2(4\pi - 3\sqrt{3})$; a_+ is the three-body parameter ($a_+ > 0$); η is the inelasticity parameter, where $\eta \ll 1$ means low decay probability into deep dimers and $\eta \gg 1$ high decay probability; and the mass-dependent coefficient is denoted by $C(\delta)$. We present results for three-body recombination rates L_3 rather than the event rate constant $\alpha_{\rm w} = L_3/2$, which takes into account that two identical atoms are taking part in the collision. Reference [47] provides the analytical formula for the mass coefficient,

$$C(\delta) = \frac{(1+\delta)^2\arcsin[1/(1+\delta)] - \sqrt{\delta(2+\delta)}}{2(4\pi - 3\sqrt{3})}, \tag{B2}$$

which is valid for $\delta > 2$. The universal rate for recombination into deep dimers is given by

$$L_3^{\rm d} = 2C(\delta)\frac{D\coth(\pi s_0)\cosh(\eta)\sinh(\eta)}{\sinh^2(\pi s_0 + \eta) + \cos^2[s_0\ln(a_{BX}/a_+)]}\frac{\hbar a_{BX}^4}{m_X}. \tag{B3}$$

For $a_{BX} > 0$, the Efimov state is expected to unbind into the Feshbach dimer at a_+, while successive Efimov levels cross the atom-dimer threshold at scattering lengths that are separated by the universal factor e^{π/s_0}. The interference between the decay pathways produces the characteristic log-periodic suppression of the three-body recombination rate, which is described by trigonometric factors $\sim \sin^2[s_0\ln(a_{BX}/a_+)]$ and $\sim \cos^2[s_0\ln(a_{BX}/a_+)]$. For our heteronuclear system, we obtain $s_0 \approx 0.03562$, corresponding to $e^{\pi/s_0} \approx 2\times 10^{38}$. Consequently, the log period is very large, and the oscillations are inaccessible within any numerically feasible range of a_{BX}. Furthermore,

the value of a_+ cannot be reliably determined in our range of L_3 calculations, because the Efimov trimer actually does not unbind into the atom-dimer threshold, as presented in Fig. 2(c). Thus, we treat the trigonometric factors as effectively constant. We propose that the interference terms $\sim \sin^2[s_0 \ln(a_{BX}/a_+)]$ and $\sim \cos^2[s_0 \ln(a_{BX}/a_+)]$ are set to 1 and 0, respectively. We emphasize that this approach represents a limiting-case approximation rather than a general prediction. In this way, however, we capture the universal scaling behavior of Efimov-related interferences by introducing a *maximum amplitude* for recombination into a weakly bound Feshbach molecular state, which is given by

$$A(L_3^{\mathrm{w}}) = 2C(\delta)\frac{D(1+\sinh^2\eta)}{\sinh^2(\pi s_0+\eta)}\frac{\hbar a_{BX}^4}{m_X}. \tag{B4}$$

Similarly, the maximum amplitude for recombination into deep dimers is given by

$$A(L_3^{\mathrm{d}}) = 2C(\delta)\frac{D\coth(\pi s_0)\cosh(\eta)\sinh(\eta)}{\sinh^2(\pi s_0+\eta)}\frac{\hbar a_{BX}^4}{m_X}. \tag{B5}$$

Naturally, the formula for the total recombination rate is, therefore, given by

$$A(L_3) = A(L_3^{\mathrm{w}}) + A(L_3^{\mathrm{d}}). \tag{B6}$$

We fit the model presented in Eq. (B6) to our numerical results and estimate the value $\eta \approx 0.027$.

Three-body recombination for $a_{BX} < 0$—For $a_{BX} < 0$, shallow Feshbach dimers are absent. The atoms can only recombine into deep dimers. Following Ref. [47], the rate constant for the recombination into deep dimers is given by

$$L_3^{\mathrm{d}} = C(\delta)\frac{D\coth(\pi s_0)\sinh(2\eta)}{\sinh^2(\eta)+\sin^2[s_0\ln(a_{BX}/a_-)]}\frac{\hbar a_{BX}^4}{m_X}, \tag{C1}$$

where a_- is the position of the Efimov resonance. Using limited data for the numerically calculated L_3 (obtained up to $|a_{BX}| < 100 r_{\mathrm{vdW}}$) we give a very rough estimate that $a_- \approx -200\, r_{\mathrm{vdW}}$. Although $|a_-|$ is substantially smaller than a_+, the numerical limit of our calculations does not allow us to confidently include the term $\sin^2[s_0 \ln(a_{BX}/a_-)]$ in our model for fitting. Instead, we follow the approach given for $a_{BX} > 0$ and compare our results to the maximum amplitude of the three-body recombination

$$A(L_3) = C(\delta)\frac{D\coth(\pi s_0)\sinh(2\eta)}{\sinh^2(\eta)}\frac{\hbar a_{BX}^4}{m_X}. \tag{C2}$$

The fit of this model to numerical values allows us to approximate the value $\eta \approx 0.17$.

Supplemental Material for "Universality in Ionic Three-body Systems Near an Ion-atom Feshbach Resonance"

Jacek Gębala,[1] Michał Tomza,[1] and José P. D'Incao[2,3]

[1]*Faculty of Physics, University of Warsaw, Pasteura 5, 02-093 Warsaw, Poland*
[2]*JILA, NIST, and the Department of Physics, University of Colorado, Boulder, CO 80309, USA*
[3]*Department of Physics, University of Massachusetts Boston, Boston, MA 02125, USA*

(Dated: June 4, 2026)

The adiabatic hyperspherical representation

We solve the three-body problem by employing the adiabatic hyperspherical representation [1]. Within this framework, the motion of the three-body system can be separated into the hyperradial and hyperangular parts. The hyperradius R determines the overall scale of the system, while the remaining degrees of freedom are captured by a set of hyperangles Ω, which describe both the internal motion and the system's rotations.

Upon rescaling the total wavefunction using the appropriate asymptotics $\Psi = \psi/R^{5/2}$ and separating out the center-of-mass motion, the three-body Schödinger Equation can be written in the following form

$$\left[-\frac{\hbar^2}{2\mu}\frac{\partial^2}{\partial R^2} + \hat{H}_{\rm ad}(R,\Omega)\right]\psi(R,\Omega) = E\psi(R,\Omega)\ , \tag{1}$$

where the adiabatic Hamiltonian, $\hat{H}_{\rm ad}$, is given by

$$\hat{H}_{\rm ad} = \frac{\Lambda^2(\Omega)+15/4}{2\mu R^2} + V(R,\Omega)\ . \tag{2}$$

The hyperangular part of the kinetic energy as represented by the grand-angular momentum operator, $\Lambda^2(\Omega)$, and $V(R,\Omega)$ is the three-body interaction potential.

The adiabatic separability of the hyperradial and hyperangular motion of the three-body system allows us to impose the adiabatic expansion on the total wavefunction

$$\psi_\nu(R,\Omega) = \sum_\nu F_\nu(R)\Phi_\nu(R;\Omega)\ , \tag{3}$$

where $F_\nu(R)$ are the hyperradial wavefunctions, $\Phi_\nu(R;\Omega)$ are the channel functions, and ν represents the set of quantum numbers describing each channel. The channel functions form an orthonormal basis of the expansion and are the solutions of the adiabatic equation

$$\hat{H}_{\rm ad}\Phi_\nu(R;\Omega) = U_\nu(R)\Phi_\nu(R;\Omega)\ , \tag{4}$$

at fixed R, where $U_\nu(R)$ are the three-body hyperspherical potentials.

Using the adiabatic expansion, we obtain the hyperradial Schrödinger Equation. It is a set of coupled differential equations, which allow us to find the hyperradial wavefunctions $F_\nu(R)$

$$\left[-\frac{\hbar^2}{2\mu}\frac{d^2}{dR^2} + U_\nu(R) - E\right]F_\nu(R) + \sum_{\nu'} W_{\nu\nu'}(R)F_{\nu'}(R) = 0\ . \tag{5}$$

The hypperradial Schrödinger Equation describes the motion of the three-body system governed by the three-body effective potential matrix $W_{\nu\nu'}(R)$ defined by

$$W_{\nu\nu'}(R) = 2P_{\nu\nu'}(R)\frac{d}{dR} + Q_{\nu\nu'}(R)\ . \tag{6}$$

The derivative couplings $P_{\nu\nu'}(R)$ and $Q_{\nu\nu'}(R)$ are given by

$$\begin{aligned} P_{\nu\nu'}(R) &= -\frac{\hbar^2}{2\mu}\left\langle\Phi_\nu(R)\middle|\frac{\partial\Phi_{\nu'}(R)}{\partial R}\right\rangle \\ Q_{\nu\nu'}(R) &= -\frac{\hbar^2}{2\mu}\left\langle\Phi_\nu(R)\middle|\frac{\partial^2\Phi_{\nu'}(R)}{\partial R^2}\right\rangle \end{aligned}\ , \tag{7}$$

where the brackets denote integrating over the hyperangles. The first derivative coupling is zero, $P_{\nu\nu}(R) = 0$, for $\nu' = \nu$ due to the orthonormality of the channel functions $\Phi_\nu(R)$. Thus, the diagonal part of the $W_{\nu\nu}(R)$ matrix is equal to the nonadiabatic coupling $Q_{\nu\nu}(R)$.

Evidence of universality in ion-atom-atom systems

In our studies, we have explored the combination of various LiLi and $LiBa^+$ interaction models supporting different number of s-wave bound states. Although not strictly necessary for universality studies, we chose to display results obtained from the model where the Li-Li and Li-Ba^+ interactions support, respectively, 2 and 6 s-wave states because it more closely represents the real physics of the problem. Due to the largely different characteristic energy scales for the Li-Li and Li-Ba^+ interactions ($E_{\rm vdW}^{\rm LiLi}/E_* \approx 10^3$), it takes a Li-$Ba^+$ interaction supporting more states than the Li-Li to provide a similar strength at short distances. This ensures that Li-Li and Li-Ba^+ bound states overlap, leading to deeply bound three-body potentials associated with the $LiBa^+$ dimer channels comparable to those corresponding to the Li_2 dimers.

For universality studies near a Li-Ba^+ Feshbach resonance ($|a_{BX}|/r_* \gg 1$), it is crucial to compare results obtained from Li-Li and Li-Ba^+ model interactions including different number of bound states, as they produce drastically different short-range physics. In order to further test universality, it is also important to explore Li-Li interaction models producing different scattering lengths, a_{BB}, to understand the impact of the interaction between neutral atoms in an ionic three-body problem.

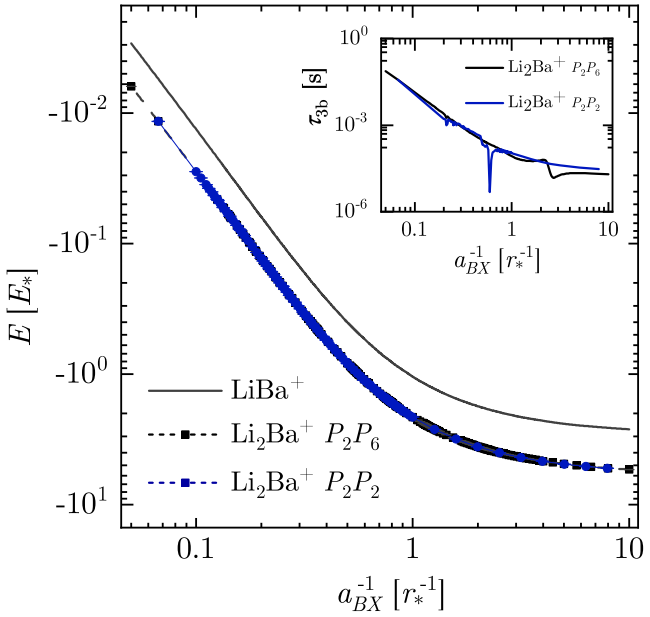

FIG. S1. Energy of the lowest Efimov state and the corresponding width Γ expressed as error bars for LiLiBa$^+$ calculated for two interacting models supporting m BB s-wave bound states and n BX s-wave bound states – marked 'P_mP_n'. The inset shows the lifetime $\tau = \hbar/\Gamma$ of the Efimov states for LiLiBa$^+$ for both of the interaction models. The perturbation of the lifetime of the Efimov state at $a_{BX} \simeq 1$ is a result of the three-body state interference with a high-partial wave diatomic molecular state.

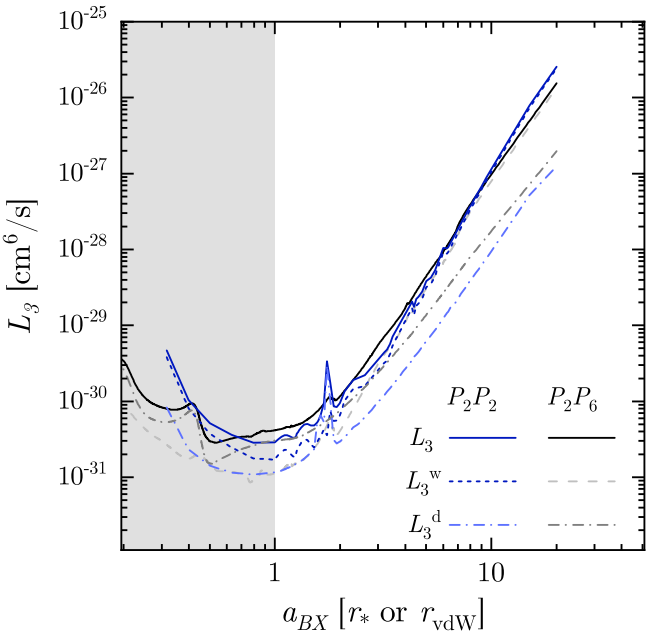

FIG. S2. (a), (b) Three-body recombination rate L_3 and partial rates $L_3^{\rm w}$ and $L_3^{\rm d} = L_3 - L_3^w$ for LiLiBa$^+$ calculated for two interacting models: P_2P_2 and P_2P_6'. For small values of $|a_{BX}| \lesssim r_*$, L_3 display non-universal resonant effects associated with high-partial waves diatomic molecular states [2], some of which are not resolved in the figure.

In Fig. S1 we provide evidence of LiLiBa$^+$ universality by comparing the energy of the lowest Efimov state obtained from $P_{n_s}P_{n_s^+}$ model interactions supporting different number of Li$_2$ and LiBa$^+$ s-wave bound states, n_s and n_s^+, respectively. The relative variations between the energies obtained from the two models remain within 2% for the range of scattering lengths shown in Fig. S1. We note that both models also present similarly long lifetimes for Efimov states, allowing us to point out the extended lifetimes in the ionic three-body systems as another universal property in the problem. Below, we will present our theoretical understanding of the physics leading to such universal properties while discussing the properties of the three-body effective potentials associated with the Efimov physics.

Similarly, we have investigated manifestations of universality in LiLiBa$^+$ recombination. However, we find that such signatures are considerably more subtle and difficult to realize to the same degree as those observed in the energy spectrum. In Fig. S2, we present our results for the three-body recombination rate $L_3(a_{BX} > 0)$ obtained from the P_2P_2 and P_2P_6 models, together with the corresponding partial contributions from recombination into the weakly bound LiBa$^+$ s-wave state, L_3^w, and into the remaining deeply bound channels, $L_3^d = L_3 - L_3^w$. While a degree of universality is indirectly reflected in L_3^d, the clearest signatures for $a_{BX} > 0$ emerge through L_3^w, particularly in the limit $\eta \to 0$, where $L_3^d \to 0$. In our calculations, however, $\eta \neq 0$, and although the behavior of L_3 may not appear at first sight as strong evidence of universality, we argue it remains fully consistent with it.

The main challenge in probing universality via L_3 in a system with an unfavorable mass ratio, $m_B/m_X \ll 1$, such as ours, stems from the extremely weak Efimov attraction characterized by $s_0 \approx 0.03562$. This leads to an extraordinarily large geometric scaling parameter, $e^{\pi/s_0} \approx 2\times10^{38}$, characterizing the log-periodic occurrence of Efimov features ($a_- < 0$ corresponding to resonances and $a_+ > 0$ to interference minima) in L_3. This has primarily two effects. First, within the framework in which the three-body parameters a_- and a_+ are universally set by the short-range length scale r_* –analogous to the familiar $|a_-| \approx 10\,r_{\rm vdW}$ relation for identical bosons for which $e^{\pi/s_0} \approx 22.7$– the weakness of the Efimov interaction implies that both a_- and a_+ should likely be expected to occur at values much larger than $10\,r_*$. Second, the enormous scaling factor e^{π/s_0} indicates that the characteristic range in a_{BX} over which a given Efimov feature develops is itself vastly expanded compared to the identical-boson case. Consequently, resolving universal behavior would require variations of a_{BX} over many orders of magnitude.

The limited interval accessible in our calculations ($|a_{BX}| \leq 20r_*$) is therefore insufficient to clearly reveal such universality. [Note that $|a_{BX}| = 20r_*$ is by no means small in absolute terms, corresponding to $|a_{BX}| \approx 440\,r_{\rm vdW} \approx 1.4\times10^4\,a_0$ where $r_{\rm vdW}$ is the van der Waals length for the Li–Li inter-

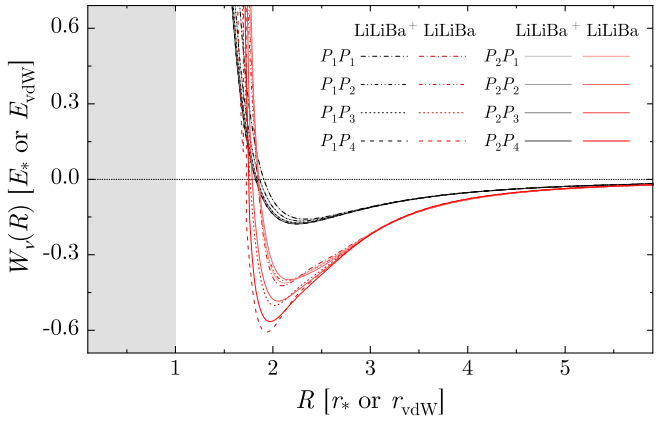

FIG. S3. Three-body effective potential, $W_\nu(R) = U_\nu(R) + W_{\nu\nu}(R)$, for the Efimov channel at $a_{BX} \to \infty$, for the LiLiBa$^+$ (tones of gray) and LiLiBa (tones of red) systems presented in relative units. The potentials are calculated for P_2P_n interaction models (n = 1 to 4). The value of a_{BB} is set to the background scattering length for ^{7}Li atoms ($a_{BB} = -27.3a_0$).

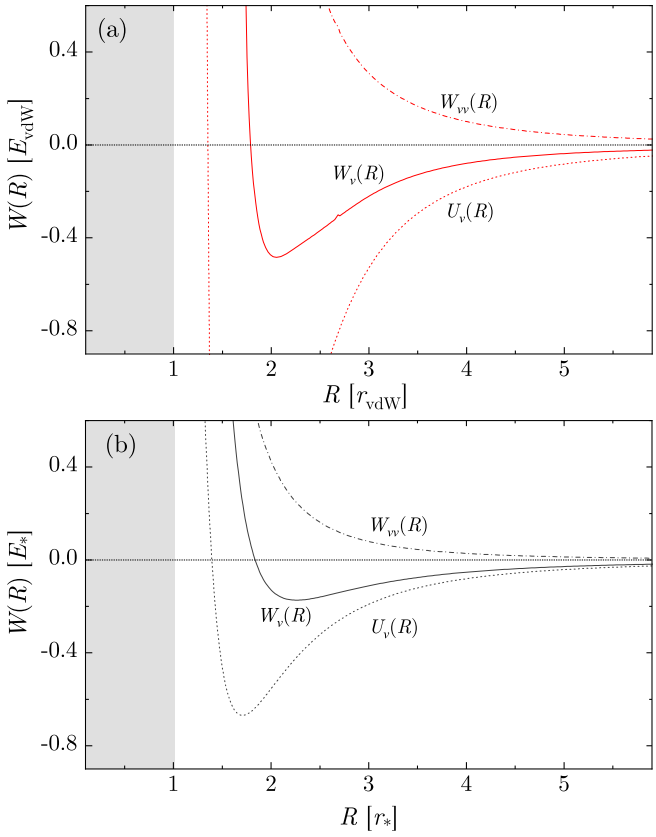

FIG. S4. The three-body hyperspherical potentials $U_\nu(R)$ and the diagonal parts of the three body effective potential matrix $W_{\nu\nu}(r)$, as well as the three-body effective potentials $W_\nu(R) = U_\nu(R) + W_{\nu\nu}(R)$ for the Efimov channel at $a_{BX} = \pm\infty$, for the (a) LiLiBa and (b) LiLiBa$^+$ system calculated using the P_2P_3 interaction model.

action.] As a result, our calculations explore an extremely small fraction of a period of log-periodic behavior of L_3 and a modest variations of η, representing differences from distinct model interactions, can produce substantial changes within this restricted range of a_{BX}. For instance, using Eq. (7) for L_3^w in the main text, setting $a_+ = 100r_*$, the values of L_3^w obtained using $\eta = 0.1$ and $\eta = 0.125$ can differ between 42%-76% for values of a_{BX} within the $[r_*,20r_*]$ range, i.e., away from $a_{BX} = a_+$. A much smaller variation in L_3^w is observed for values of $s_0 > 1.00624$ corresponding to the cases with three identical bosons and systems with a favorable mass ratio, $m_B/m_X \gg 1$, thus indicating a stronger sensitivity to η for systems with $m_B/m_X \ll 1$. In this context, we believe the level of variations observed for L_3 shown in Fig. S2 is still consistent with universal behavior, although not enough to make a claim nearly as strong as that found for the energies of the Efimov states in Fig. S1.

Mechanism of universality in ion-atom-atom systems

Similar to the universality with neutral atoms, we have found that the hallmark of universality in strongly interacting ionic three-body systems is also a repulsive barrier in the effective three-body potential describing Efimov physics, which prevents atoms from reaching short distances and probing non-universal effects. In Fig. S3 we demonstrate this and compare the effective potentials $W_\nu(R) = U_\nu(R) + W_{\nu\nu}(R)$ for both LiLiBa (tones of red) and LiLiBa$^+$ (tones of gray) systems with $a_{BX} = \pm\infty$ and a_{BB} set to the Li-Li background value, $a_{BB} = -27.3a_0$. These results were obtained from different model potentials (P_1P_n and P_2P_n, with n = 1 to 4) and are presented in relative units. In both neutral and ionic cases there exist a repulsive barrier preventing atoms to approach short distances defined in each case by the corresponding characteristic range of the interactions–$R/r_{\rm vdW} \lesssim 2$ for neutral and $R/r_* \lesssim 2$ for ionic systems.

Although Fig. S3 indicates that both strongly interacting neutral and ionic three-body systems are universal, there are a few key differences that make ionic systems unique. It is clear from Fig. S3 that the strength of the effective interaction is deeper (in relative units) for neutral atoms than for ionic systems, near the corresponding equilibrium positions, $R \approx 2r_{\rm vdW}$ and $R \approx 2r_*$, respectively. More importantly, neutral potentials change faster as R approaches short-distances than ionic potentials. In the adiabatic representation, fast changes in R are associated with the increase of non-adiabatic effects. In fact, in Fig. S4 we show the non-adiabatic effects in the effective potentials $W_\nu(R) = U_\nu(R)+W_{\nu\nu}(R)$ originated from the diagonal non-adiabatic coupling, $W_{\nu\nu}(R)$. This figure clearly shows that three-body interactions $U_\nu(R)$ varies much faster for neutral [Fig. S4(a)] than for ionic [Fig. S4(b)] systems, which leads to much larger diagonal non-adiabatic couplings $W_{\nu\nu}$.

In fact, since in hyperspherical representation inelastic transitions are driven exclusively from non-adiabatic couplings $W_{\nu\nu'}(R)$ [see Eq. (6)], the suppression of non-adiabatic ef-

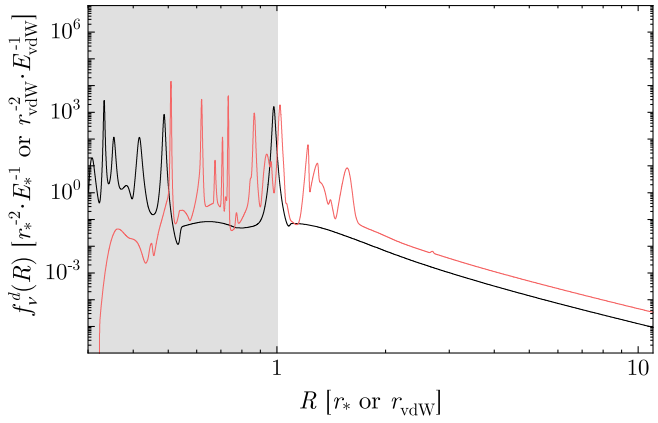

FIG. S5. The sums of non-adiabatic couplings between the Efimov channel and all deeply bound states $f_\nu^d(R)$ for the LiLiBa (red) and LiLiBa$^+$ (black) systems calculated using the P_2P_3 interaction model.

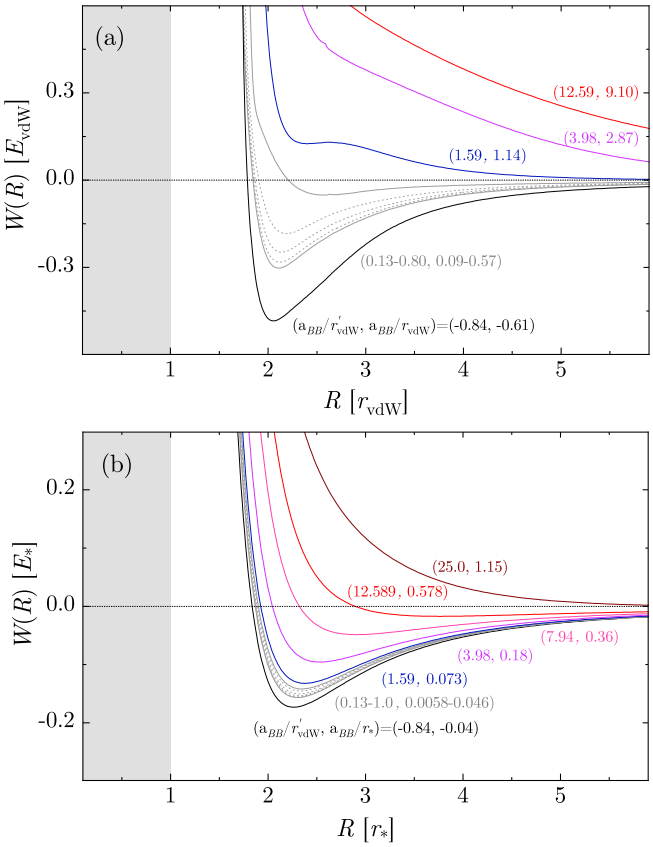

FIG. S6. Three-body effective potential $W(R)$ for the Efimov channel at $a_{BX} = \pm\infty$, for the (a) LiLiBa and (b) LiLiBa$^+$ system calculated using the P_2P_3 interaction model. The potentials are calculated for many values of a_{BB} ranging from $-0.84035r'_{\rm vdW}$ $(-0.039r_*)$ to $25r'_{\rm vdW}$ $(1.149r_*)$, where $r'_{\rm vdW}$ is the van der Waals length related to the BB interaction.

fects for ionic systems (relative to neutral systems) has a profound impact on various relevant observables. In our case, we are mostly interested in three-body observables for processes that involve the Efimov channel. In particular, the non-adiabatic couplings between this channel and deeply bound diatomic channels control the amplitude of recombination as well as the lifetime of Efimov states. As a result, characterizing such non-adiabatic effects can potentially elucidate important properties of the system. For each pair of channels ν and ν', the strength of the non-adiabatic coupling is characterized by

$$f_{\nu\nu'}(R) = \frac{\hbar^2}{2\mu}\frac{P^2_{\nu\nu'}(R)}{|U_\nu(R) - U_{\nu'}(R)|}, \tag{8}$$

where $P_{\nu\nu'}(R)$ is the first-order non-adiabatic coupling [see Eq. (7)]. However, for systems containing various bound states, the number of channels that contribute to the inelastic transitions can be quite large. In order to encapsulate the overall effect of all relevant transitions, we define the strength of the non-adiabatic couplings between the Efimov channel, ν, with the deeply bound diatomic channels, ν', by summing over all channels ν',

$$f_\nu^d(R) = \sum_{\nu'} f_{\nu\nu'}(R). \tag{9}$$

In Fig. S5, we show the effective coupling strength, $f_\nu^d(R)$, for both LiLiBa and LiLiBa$^+$ systems, emphasizing the suppression of non-adiabatic effects for ionic systems. For large values of R, $f_\nu^d(R)$ falls off as $1/R^3$ [3] for both neutral and ionic systems, however, with an amplitude for ionic systems that is a factor 4 smaller than for neutrals. As R approaches short distances, $f_\nu^d(R)$ for neutral systems display various enhancements for $R/r_{\rm vdW} \lesssim 2$ associated to avoid -crossings characteristic of heteronuclear neutral atom systems [4], while $f_\nu^d(R)$ for ionic systems remains smooth, and with a significant smaller amplitude, until $R/r_* \lesssim 1$. While we associate this suppression of non-adiabatic transitions with the long lifetimes for ionic Efimov states, the suppression of the ionic recombination L_3 is likely a combination of changes in the long-range diagonal nonadiabatic coupling [see Figs. S4(a) and (b)] and off-diagonal non-adiabatic couplings represented in Fig. S5.

It is also crucial to emphasize the role of the intraspecies scattering length a_{BB} in the universal properties of a heteronuclear BBX system with large a_{BX} scattering length. The importance of a_{BB} in neutral atoms systems is a well known result [5–7] and evidently should play a similar role in our ionic three-body system, LiLiBa$^+$. For neutral atoms BBX systems with strong interspecies vdW interactions, $|a_{BX}| \gg r^{BX}_{\rm vdW}$, universality should in general be determined in terms of characteristic range on the interactions, $r^{BX}_{\rm vdW}$. However, whenever $|a_{BB}| \gtrsim r^{BX}_{\rm vdW}$, BBX universality is expected now to be determined in terms of a_{BB}. In the numerical studies of Ref. [5] [see Fig. 2 of this reference], for instance, noticeable changes on the Efimov states at $a_{BX} = \pm\infty$ are observed for values of $|a_{BB}| \gtrsim 0.26r^{BX}_{\rm vdW}$, which is a small number (in absolute units).

However, there is a fundamental difference between what is found for neutral atoms and our studies. For ionic systems, universality is set in terms of the characteristic range of the atom-ion (BX) interaction, r_*, which is typically much larger than neutral atoms short-range length scales ($r_{\rm vdW}^{BB}$ or $r_{\rm vdW}^{BX}$). In this case, the expectation is that it would require a larger value for a_{BB} (in absolute units) for changes in universality to take place than what is found for neutral atoms systems. This effect can be seen in Fig. S6, where we show the effective potentials for LiLiBa$^+$ with $a_{BX} = \pm\infty$ and different values of a_{BB}, displayed in the figure in units of $r_* \approx 707.03a_0$, for the LiBa$^+$ (BX) interaction, and $r_{\rm vdW} \approx 32.8a_0$, for the LiLi ($BB$) interaction. Figure S6 shows that changes beyond 15% on the three-body interactions near its minimum are observed for $a_{BB} \gtrsim 3.981 r_{\rm vdW} = 0.183 r_*$, a point where a_{BB} should become the dominant length scale characterizing universality in the problem. Since changes in the depth of the three-body potentials do not directly translate, for instance, into changes on the energies of the Efimov states [in Ref. [8] it was found that changes of about 30% on the minimum of the potential caused less than 10% variation of the energy of a Efimov state], a more quantitative analysis is required in order to quantify the effects of changes of a_{BB} in the universal properties of the system. Nevertheless, Fig. S6 qualitatively shows that a_{BB} also plays a role in the universality in ionic three-body systems, but in a less critical way than found for neutral atoms. While for ionic systems BBX universality is insensitive to the BB interaction for $|a_{BB}| \lesssim r_*$, therefore allowing for large values and variations of a_{BB}, for neutral systems BBX universality is substantially modified for much smaller values of $|a_{BB}| \gtrsim r_{\rm vdW}^{BX}$.

[1] J. Wang, J. P. D'Incao, and C. H. Greene, Numerical study of three-body recombination for systems with many bound states, Phys. Rev. A **84**, 052721 (2011).

[2] J. Wang, J. P. D'Incao, Y. Wang, and C. H. Greene, Universal three-body recombination via resonant d-wave interactions, Phys. Rev. A **86**, 062511 (2012).

[3] J. P. D'Incao and B. D. Esry, Manifestations of the Efimov effect for three identical bosons, Phys. Rev. A **72**, 032710 (2005).

[4] Y. Wang, J. P. D'Incao, and B. D. Esry, Cold three-body collisions in hydrogen–hydrogen–alkali-metal atomic systems, Phys. Rev. A **83**, 032703 (2011).

[5] Y. Wang, J. Wang, J. P. D'Incao, and C. H. Greene, Universal three-body parameter in heteronuclear atomic systems, Phys. Rev. Lett. **109**, 243201 (2012).

[6] S. Häfner, J. Ulmanis, E. D. Kuhnle, Y. Wang, C. H. Greene, and M. Weidemüller, Role of the intraspecies scattering length in the efimov scenario with large mass difference, Phys. Rev. A **95**, 062708 (2017).

[7] K. Oi, P. Naidon, and S. Endo, Universality of Efimov states in highly mass-imbalanced cold-atom mixtures with van der Waals and dipole interactions, Phys. Rev. A **110**, 033305 (2024).

[8] J. Wang, J. P. D'Incao, B. D. Esry, and C. H. Greene, Origin of the three-body parameter universality in Efimov physics, Phys. Rev. Lett. **108**, 263001 (2012).